nature communications

Article

https://doi.org/10.1038/s41467-025-60111-x

Atom economic closed-loop recycling of thermoset polyurethane foams

Received: 28 September 2024

Accepted: 15 May 2025

Published online: 02 June 2025

Check for updates

Zenghe Liu[1,3], Ling Liu[1,3], Yangfei Li[1], Kexuan Yang[2], Sujing Li[2], Wei Li[2], Yutian Zhu[1] ✉ & Tao Xie[2] ✉

Thermoset polyurethane foams are extensively used in industrial and consumer products, but their end-of-life recycling has been a long-standing challenge. Closed-loop recycling represents an idea solution, but its practical value is often compromised due to the consumption of catalyst and/or solvent as well as degradation in the recycled material properties. Here, we report an efficient foam-to-foam closed-loop recycling strategy that addresses these issues. Our approach relies on the inherent equilibrium nature of the covalent bonds in the polyurethane network. Addition of acetoxime shifts the equilibrium to dissociate the covalent bonds, which transforms a monolithic foam into surface functionalized micro-particles. By removing acetoxime via evaporation, the original covalent bonds are reformed and these micro-particles are rejoined to form a new foam with acetoxime as the porogen. The process employs neither catalyst nor solvent and the only chemical reagent involved (acetoxime) is fully recoverable. Importantly, the process yields new foams with mechanical properties identical or even superior to the original foam. Our strategy of achieving atom economic recycling of polyurethane foams is potentially applicable to other thermosets.

The outstanding mechanical properties and dimension stability of thermoset polymers have made them uniquely suited for many demanding applications. Among them, thermoset polyurethane foams (PUF) are widely used in industrial and consumer products including car seats, furniture, packaging, and insulation board. The worldwide annual production of PUF in 2022 is 14 million tons, occupying 67% of the polyurethane market, 50% of the polymeric foam market, and 20-30% of the total thermoset market[1–3]. With its low density, the volumetric annual production of PUF stands at an astonishing level of 0.4 billion cubic meters[4], which contributes to increasing environmental concerns after its service life[5,6]. Currently, PUF wastes are mostly landfilled or incinerated, two practices that cause secondary pollution in addition to resource wasting.

Recycling is a challenging task given the thermoset nature of PUF. Nevertheless, many attempts have been made in the past decades[7,8]. Physical recycling utilizing grounded particles as fillers is easy to implement, but has not captured much attention due to the low economical value. For chemical recycling, the concept of breaking the network bonds via glycolysis to recover the original polyol monomer has been extensively investigated for decades by both academic and industrial labs[9]. This approach employs harsh chemical conditions and consumes chemical reagents. In addition, it typically recovers only partially the polyol, which requires further purification before reuse. Consequently, the cost of recycling does not compensate its economical gain. Employing dynamic bonds can enable molecular network rearrangement, shape reconfiguration, depolymerization and regeneration capabilities for materials[10,11]. Unfortunately, the chemistries are not suitable to commodity PUF. Catalytic activation of the dynamic urethane bonds[12,13] enables direct thermal extrusion of waste foams into new films or foams, but it consumes additional reagents

[1]Key Laboratory of Organosilicon Chemistry and Material Technology, Ministry of Education, Zhejiang Key Laboratory of Organosilicon Material Technology, College of Material, Chemistry and Chemical Engineering, Hangzhou Normal University, Hangzhou, China. [2]State Key Laboratory of Chemical Engineering, College of Chemical and Biological Engineering, Zhejiang University, Hangzhou, China. [3]These authors contributed equally: Zenghe Liu, Ling Liu. ✉e-mail: ytzhu@hznu.edu.cn; taoxie@zju.edu.cn

such as catalyst and blowing agent. We have recently reported an approach for chemical upcycling of PUF into high performance 3D printable photo-resins[4]. Our approach decomposes the PUF into reworkable oligomeric fragments instead of the monomeric polyol, which are further functionalized to yield photo-curable resins. The process is conducted under mild condition and the PUF waste is fully reused without requiring purification, and the recycled product in the form of 3D printing photo-resin has significant value gain. Although the solvent (DMF) and catalyst used in such a process are fully recoverable, additional fresh monomers (around 30%) are required to tune the properties of the product(s). Despite the economic value gain associated with the upcycling, the potential consumption of the PUF waste as 3D printing resins is somewhat limited before 3D printing becomes main-stream. Consequently, the approach cannot be a realistic solution to PUF recycling in the short term.

All the above methods employ/consume multiple chemical reagents (degradation agent, curing agent, solvent, additional monomers, catalyst and/or blowing agent). We envision that a more ideal approach is to employ a single chemical reagent that can not only perform all the required functions but also be fully recoverable. This would enable foam to foam recycling in a simple, efficient, yet atom economic manner. We hypothesize that this can be potentially realized by exploring the inherent equilibrium nature of the covalent bonds in the PUF network. Addition of a suitable reagent can shift the equilibrium to dissociate the covalent bonds, which can transform a monolithic foam into a reworkable state. By removing and recovering the chemical reagent, the original covalent bonds are reformed. If this chemical reagent can also function as a porogen, no additional foaming agent would be required. We describe hereafter our successful attempt in this direction, achieving foam to foam recycling in an atom economic fashion using acetoxime as the sole recoverable chemical reagent.

Results and discussion

Design principle for PUF closed-loop recycling

Polyurethane foams (PUF) are classified as rigid foams and soft foams. The former is used for thermal insulation purpose for which the thermal conductivity is the key. The latter is used for soft supports (e.g. mattresses and seat cushion) for which the mechanical properties are critical. We focus on the latter in this study. The commercial soft PUF used in this study is identical to what is described in our previous publication[4]. It is a crosslinked network with urea, urethane, and biuret bonds at a molar ratio of 3:1:0.2[4]. We note that, for commercial polyurethane foam production, isocyanates must not only react with polyols to form urethane bonds but also react with water (a blowing agent) to release CO_2 gas (for foaming), simultaneously generating substantial urea bonds and biuret bonds. Consequently, urea bond content far exceeds urethane bond content. However, it is a convention to call them polyurethane foams rather than polyurea foams.

The chemical principle behind our closed-loop recycling is schematically shown in Fig. 1. The key concept here is that, at the heated state, the urea, urethane, and biuret bonds are in their equilibrium states with the isocynate and the corresponding amine, alcohol and urea groups (Fig. 1a)[14]. Normally, the equilibria favor the associated states, namely urea, urethane, and biuret bonds. However, with the addition of an excessive amount of acetoxime, the equilibria (Fig. 1b) are pushed towards the formation of oxime-urethane[15] bonds and the network connections are broken. This would lead to the deconstruction of the PUF network. As such, the monolithic PUF can be degraded into particles decorated with surface functional groups including oxime-urethane and XH, with XH being amine, and alcohol, and urea (Fig. 1c). When acetoxime is removed, the equilibria favor the formation of the original bonds (urea, urethane, and biuret)[14,16] and these particles can be re-joined together to regenerate the original polyurethane network. In this whole process, acetoxime is the only chemical reagent involved and it is fully recovered upon process completion.

Deconstruction of PUF

As the first step, the PUF is mechanically grounded for four minutes, yielding PUF particles of diverse sizes and shapes (Fig. 2a) which are carried from the pore morphology of the initial PUF. The next step is the chemical deconstruction, at which these particles are mixed with an excessive amount of acetoxime and heated at 130 °C. At a fixed acetoxime/PUF weight ratio of 20, the particles become smaller with the deconstruction time (Fig. 2a-b). By fixing the deconstruction time at 20 min, the impact of the acetoxime/PUF ratio is investigated. The results show that the particle shape (Fig. 2c), size and their distribution (Fig. 2d) do not change notably as the acetoxime/PUF ratio increases. To further probe the chemical deconstruction mechanism, swelling of PUF in acetoxime at 130 °C is investigated. The result shows that the PUF reaches its maximum volume expansion within 5 s (Fig. 2e), implying rapid complete swelling. Judging from the actual volume change, the equilibrium volumetric swelling ratio is determined as 2.2. Since the chemical reactions occur at a much slower pace, the rapid swelling suggests that the network chemical deconstruction occurs uniformly within the PUF.

Revelation of the chemical mechanism

To understand the network deconstruction mechanism, three small molecular model compounds containing urea, urethane, and biuret bonds are individually subjected to reactions with excessive oxime at 130 °C. The details of this model compound study are presented in Supplementary Figs. 1–10 of Methods Section 'Model compound experiments'. Here, the molar ratios (oxime/urea, oxime/urethane, and oxime/biuret) are kept at 46/3, 46/1, and 46/0.2 so that they are in line with the ratio of urea/urethane/biuret (3:1:0.2) in the PUF. However, the amount of oxime was reduced by a factor of thirteen (versus the oxime content at a acetoxime/PUF weight ratio of 20) to maintain a sufficiently high concentration for ^{1}H NMR analysis. The ^{1}H NMR analysis (Fig. 3a) confirms that all these three bonds (urea/urethane/biuret) undergo thermal exchange reactions with oxime to form oxime-urethane, and the corresponding amine, alcohol, and urea. The ^{1}H NMR analysis further allows kinetic investigation of these model reactions to yield the three linear curves in Fig. 3b. Judging from the slopes of the three curves, the relative contributions to the network deconstruction follows the order of urea>urethane≈biuret. The total molar percentage of the cleaved bonds relative to the initial bonds increases linearly with time from 0% to 22.6% at 120 min (Fig. 3c). This implies that, for the PUF particles, the percentage of bond cleavage increases with the deconstruction time, accompanied by particle fragmentation (Fig. 3d). This conclusion is consistent with the results presented in Fig. 2a, b, showing that the particle size decrease with the deconstruction time. Overall, the model compound study suggests that the PUF deconstructs uniformly and linearly with time to produce particles with oxime-urethane, amine, alcohol, and urea in the network, which is in line with the scheme shown in Fig. 1c. X-ray photoelectron spectroscopy (XPS) was used to analyze the surface chemistry of PUF before and after degradation. The peak of the original PUF at 399.1 eV is attributed to C-N (Supplementary Fig. 11). After degradation by oxime, the peak shifts to 399.7 eV corresponding to the formation of C=N, which indicates the transformation of urethane/urea/biuret into oxime-urethane.

Reconstruction of PUF

Since our goal is atom economic closed-loop foam to form recycling, it is crucial to devise a mechanism to not only reconstruct the PUF molecular network but also generate porous structures, importantly without consuming any additional reagent. In the above PUF

https://doi.org/10.1038/s41467-025-60111-x

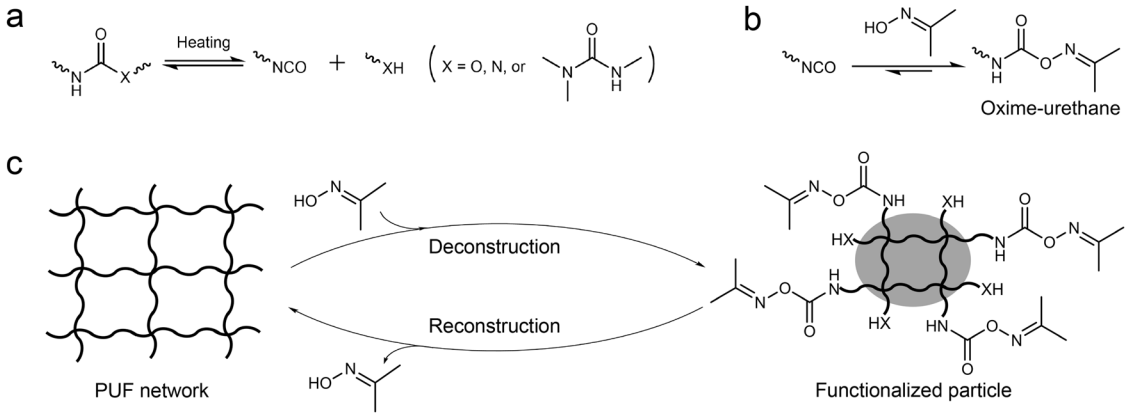

Fig. 1 | Design principle of the atom economic closed-loop recycling of polyurethane foams (PUF). a Thermal equilibria states of urea, urethane, and biuret. **b** Shifting equilibria with excessive oxime. **c** Closed-loop recycling of PUF.

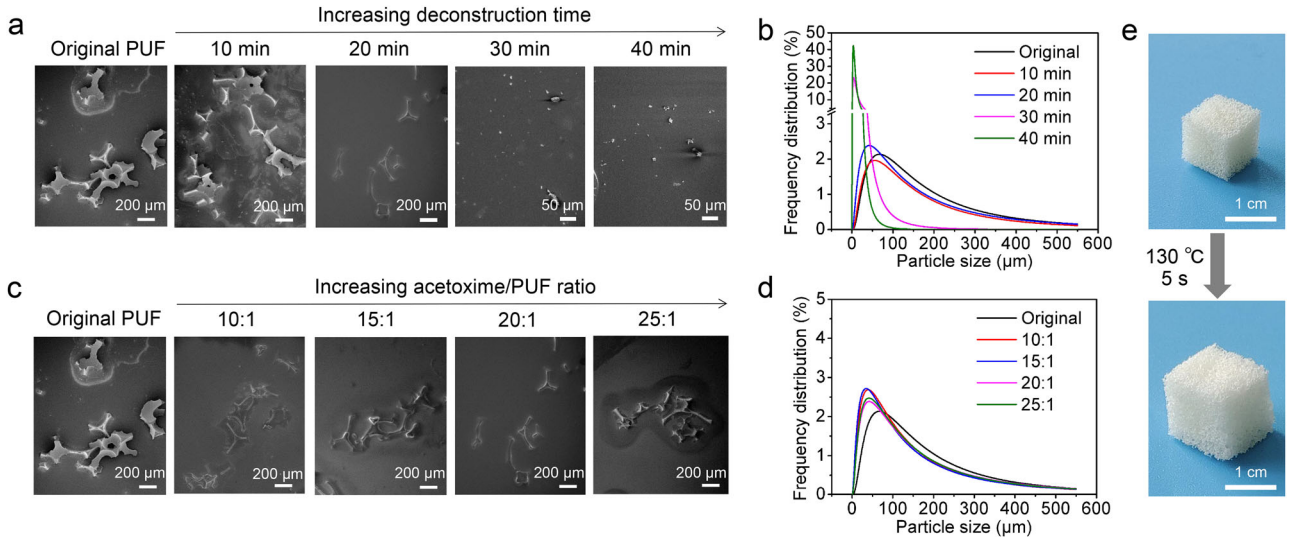

Fig. 2 | Deconstruction of polyurethane foams (PUF) into surface functionalized particles. The impact of deconstruction time on the particle (**a**) size and (**b**) morphology at a fixed acetoxime/PUF ratio of 20. The impact of acetoxime/PUF ratio on the particle (**c**) size and (**d**) morphology at a fixed deconstruction time of 20 minutes. **e** The photographs of PUF before and after swelling in acetoxime at 130 °C.

deconstruction process, acetoxime is used in a large excess in order to push the equilibria to dissociate the urethane, urea, and biuret bonds. In principle, removing all the acetoxime would push the equilibria back to the associative states to facilitate the reconstruction of the original molecular network of the PUF (Fig. 1c). However, restoring the porous structures without employing any blowing reagent presents a different challenge. We note here that acetoxime is a crystallizable compound with a melting temperature of 61 °C and it evaporates upon heating under vacuum. This presents a unique opportunity to use the excess acetoxime as a porogen to reconstruct the porosity, in a way similar to freeze-drying of water. Thus, removing and recovering acetoxime in vacuum can potentially restore the molecular structure and porous architecture simultaneously. To investigate the PUF reconstruction, we focus hereafter on the deconstruction condition of acetoxime/PUF ratio of 20 and destruction time of 20 min, with any deviation specifically noted. This condition is chosen so that the original bonds are sufficiently cleaved yet the resulting particles (Fig. 2a) largely retain the shape carried from the original foam. Another important consideration is that only loose packing is possible due to the particle shapes, which would favor pore generation. The particle/acetoxime mixture obtained under this condition is subjected to heating under vacuum to regenerate the foam. We note that vacuum evaporation and pore formation could not be achieved below the melting point of acetoxime (61 °C). This was only achieved at a temperature above the melting point (90–150 °C). In the process, we did not observe any liquid leaking. We suspect that the evaporation above the melting point is attributed to the following three factors: 1. evaporation dissipates substantial heat, preventing the material from melting; 2. Upon undergoing evaporation processing, the material's surface layer undergoes rapid cross-linking through fast evaporation, forming a polymer shell that maintains the structural integrity; 3. The depolymerization products are not molecular-level substances but rather chemically cross-linked microparticles which provide inherent self-supporting properties. Here, the time requires to reach a constant weight implies complete evaporation of acetoxime, which is defined as the evaporation time. Supplementary Fig. 12 shows that the evaporation time is notably decreased as the temperature is raised until reaching a plateau of 3 h at around 130 °C, which we fix as the standard reconstruction condition unless otherwise noted. It should be noted that the repolymerization/molding temperature coincides with the depolymerization temperature, the persistent solid-state integrity of the material attributed to the absence of acetoxime phase transition (melting) restricts molecular mobility, thereby resulting in negligible degradation. Furthermore, the reversible nature of this degradation mechanism fundamentally prevents adverse impacts on material integrity/final product performance.

https://doi.org/10.1038/s41467-025-60111-x

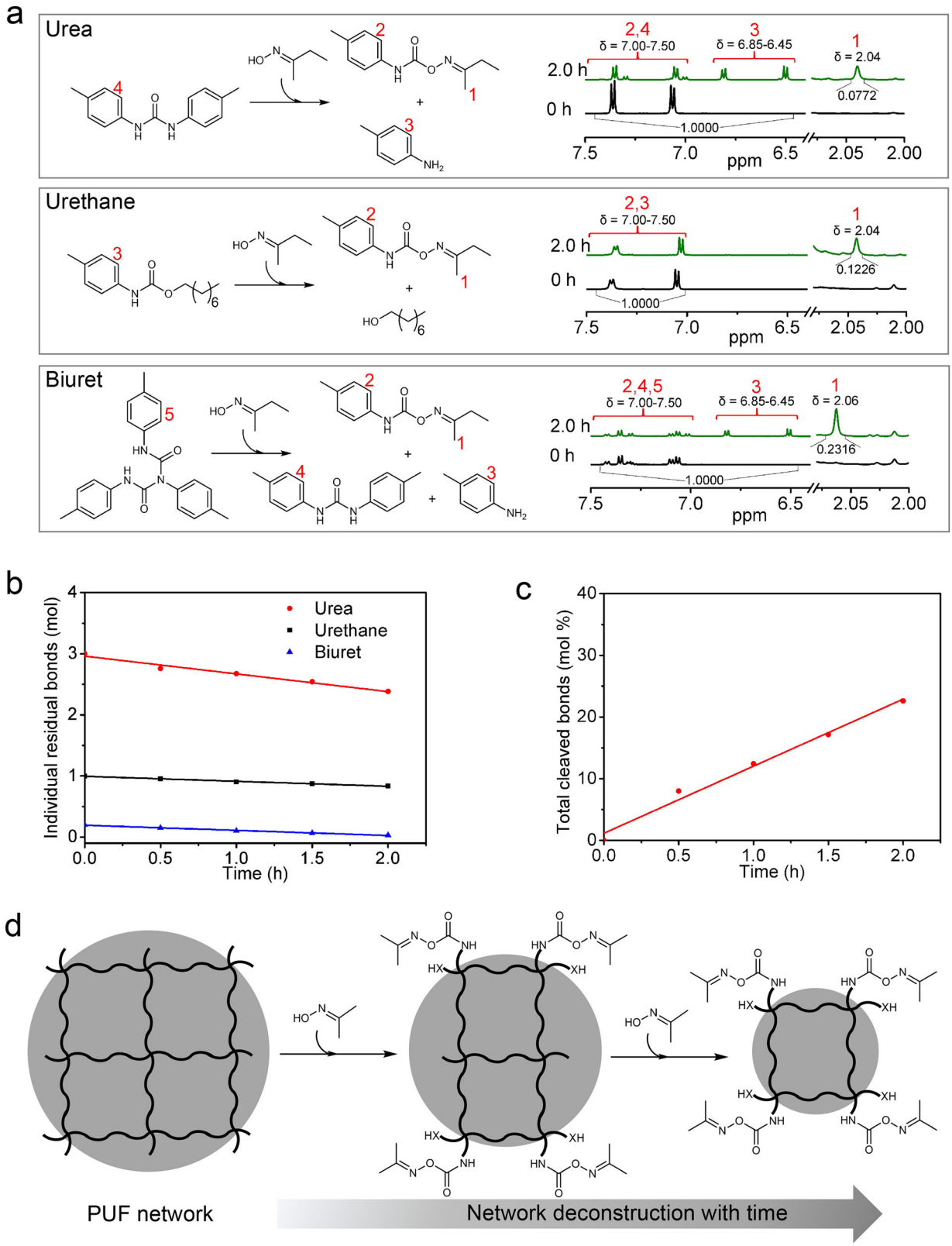

Fig. 3 | Chemical mechanisms of polyurethane foams (PUF) deconstruction. a ^{1}H NMR analyses of the thermal exchange reactions of acetoxime with urea, urethane, and biuret bonds, with the spectra corresponding to a reaction time of 2 h in all three cases. Deuterated dimethyl sulfoxide (DMSO-d6) serves as solvent for the ^{1}H NMR analysis. The total intensity of the peaks corresponding to aromatic hydrogens is set as 1, and the comparison of the intensity of the peak corresponding to CH_3 in oxime-urethane is used to calculate the conversion. **b** The individual bond reaction kinetics from NMR analyses normalized against their molar contents in the network (urea:urethane:biuret = 3:1:0.2). **c** The total cleaved urea, urethane, and biuret bonds. **d** Schematic illustration of the network structure evolution upon chemical deconstruction.

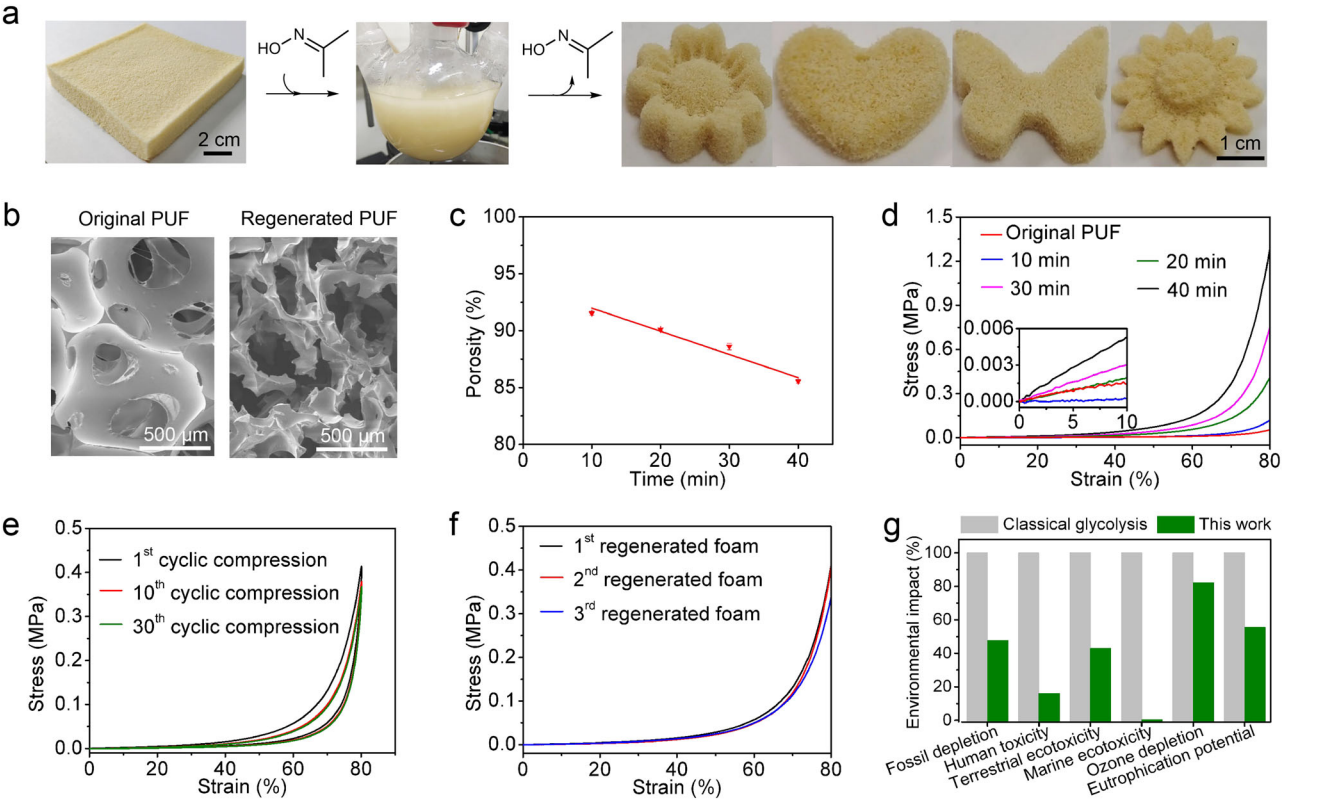

Fig. 4 | Reconstruction of polyurethane foams (PUF). a The photographs of the original PUF, the acetoxime/particle mixture after deconstruction, and the regenerated PUFs. **b** Comparison of the SEM images of the original and regenerated PUF. **c** Porosity of the regenerated PUFs corresponding to different deconstruction times. Data are presented as mean values ± standard error of the mean (s.e.m.). Centre values denote average. Error bars denote s.e.m. $n = 5$ for the samples. **d** Compressive stress-strain curves of the original and regenerated PUFs corresponding to different deconstruction times, with the insets showing the zoom-in of the small strain range. **e** The first, tenth, and thirtieth cyclic compressive stress-strain curves of the regenerated PUF. **f** Compressive stress-strain curves of the first, second, and third regenerated PUFs. **g** Comparative characterization results from life cycle assessment.

Figure 4a shows the original PUF, the acetoxime/particle mixture after deconstruction, and the regenerated PUF in different shapes as defined by the mold used. The SEM images show the porous structures of the original and regenerated PUF (Fig. 4b). Despite the big difference in pore morphology due to the different foaming techniques, the porosity of the regenerated PUF is 90%, which is slightly lower than the original foam (95%).

The FTIR spectroscopic analyses (Supplementary Fig. 13) suggest that the regenerated and the grounded PUF have same characteristic functional group peaks, especially for the carbonyl bands (urea, urethane, and biuret), verifying the re-association of the broken bonds. Compare to the original PUF, some minor new peaks appear in their FTIR spectra, which are attributed to the molecular chain scission to form some new chemical groups including hydroxyl groups under large mechanical force, heat generated, and moisture during grounding[17]. In theory, deconstructing the foam directly in the acetoxime without grounding process can prevent these side reactions scission. However, it is difficult to implement this in a laboratory setting because the macroscopic dimensions of intact foams exceed the capacity limitations of laboratory-scale reaction vessels. Consequently, we employed mechanical grounding as a necessary treatment step. Notably, this limitation can be potentially overcome in industrial-scale implementation with large capacity. Gel fraction tests suggest that their gel contents are similar at around 95%. Differential scanning calorimetry curves (Supplementary Fig. 14) show that their glass transition temperatures are identical at around −59 °C. Their thermal gravimetric analysis curves (Supplementary Fig. 15) suggest that both their thermal decomposition temperatures T_5 (the temperatures corresponding to 5% weight loss) are around 260 °C. The above results suggest that the network is reformed almost perfectly.

Although the chemical structure and the thermal properties are recovered, the mechanical performance is a different story due to the change in pore morphology, which is affected strongly by the deconstruction conditions (Supplementary Fig. 16). At the given acetoxime/PUF ratio of 20, changing the deconstruction time allows access to regenerated foams of very different mechanical characteristics. Figure 4c shows that the porosity decreases linearly from 92% to 86% as the deconstruction time increases from 10 min to 40 min. This is mainly because prolonging the deconstruction time makes the particles smaller (Fig. 2a, b), which is in favor of forming closer particle packing. The compressive mechanical performance varies drastically with the deconstruction time. Figure 4d shows that the original PUF has a linear stress-strain response in the whole strain range (up to 80%). In contrast, the regenerated PUF all exhibit strain-hardening behaviors starting at a strain around 40% and most notably at around 60%. The strain-hardening for the regenerated PUF is desirable as it would offer more mechanical support under high loads while maintaining its necessary softness at small loads. It arises from the slightly lower porosity of the regenerated foam as well as the different pore structure compared to the original foam. The inset curves in Fig. 4d show the linear small strain ranges of all the stress-strain curves. Their comparison suggests that the regenerated PUF can be either softer or stiffer than the original PUF depending on the deconstruction time. In particular, the regenerated PUF corresponding to the deconstruction time of 20 min has a modulus nearly identical to the original PUF, both at around 20 kPa. In addition to match the low strain modulus, the regenerated PUF also shows high resilience comparable to that of the

original foam as the cyclic compressive behavior suggests (Fig. 4e, Supplementary Fig. 17). Most importantly, this PUF can be repeatedly subjected to identical recycling conditions, with the mechanical properties fully maintained even after three recycling cycles (Fig. 4f). As for the density, the initial foam has a density of 0.06 g/cm^3. By comparison, the regenerated foams corresponding to the deconstruction times of 10, 20, 30, and 40 min are 0.102, 0.119, 0.137, and 0.174 g/cm^3, respectively.

Life cycle and techno-economic assessments

In the above process, acetoxime can be fully recovered at a high purity identical to the initial acetoxime (Supplementary Fig. 18) and the original PUF is fully converted into a new PUF without consuming any chemical(s). In addition, acetoxime is a low cost chemical commonly used in industry as a chemical cleaning boiler and for blocking isocyanates[16,18] and evaporation is also a common industrial practice[19–21]. We note that acetoxime is potentially carcinogenic. However, it is only used in the recycling process in which strict control can be executed to avoid human contact and its release to the environment. Since it is fully reclaimed, its presence in the final product (recycled foams) can be kept to a minimum acceptable level. Nevertheless, our overall approach of using dynamic equilibrium reactions for foam recycling can be potentially extended to reagents that are much less toxic than acetoxime, a direction we will explore in the future. Thus, our recycling process is realistic from a manufacturing standpoint. To further evaluate the impact of our recycling process on sustainability, life cycle and techno-economic assessments are conducted.

For life cycle assessment (LCA), the classical chemical recycling process based on glycolysis[6,9] is used as a control. Their system boundary and LCA network structures are illustrated in Supplementary Fig. 19, serving as the basis for the assessment. Under the assumption that the PUF is regenerated once, the LCA results obtained (Fig. 4g) suggests that our process exhibits a better overall environmental impact, with lower normalized results in fossil depletion (47.8%), human toxicity (16.1%), terrestrial ecotoxicity (43.0%), marine ecotoxicity (0.4%), ozone depletion (82.3%), and eutrophication potential (55.5%). These benefits imply that the high energy consumption due to acetoxime recovery is more than off-set by other favorable process characteristics including no by-product and no consumption of additional reagent(s). For techno-economic assessment, the total costs including raw materials and energy for our recycling process is estimated at round $0.59/kg, which is about 28.6% of that ($2.06/kg) for the classical chemical recycling method based on glycolysis (see Section 'Techno-economic analysis' in the Methods).

In summary, we demonstrate a chemical recycling process for commodity PUF based on reversibly shifting the covalent bond equilibria. This allows us to partially deconstructing the network to a reworkable state (surface functionalized particles) that enables regeneration of new PUF without consuming any chemicals (solvent, catalyst, or monomers). Our recycling process can be further improved in the future in terms of reducing the re-foaming time (limited by the evaporation speed) and more fundamentally alternative foaming techniques. Nevertheless, achieving foam to foam recycling in an atom economic fashion is attractive both economically and environmentally, pointing to a promising direction in future sustainable development of other industrial thermosets.

Methods

Materials and general measurements

Materials. Acetoxime was purchased from Macklin. 2-Butanone oxime was purchased from Meryer. *p*-Tolyl isocyanate, *p*-toluidine, and 1-octanol were all obtained from TCI. Tetrahydrofuran (THF) was purchased from Sinopharm. The commodity PUF was obtained from the production line of UE Furniture Co., Ltd. The PUF was made by the reaction of diisocyanates with polyether polyol (hydroxyl number: 20 mg KOH/g), diethanolamine, and water[4]. It was mechanically grinded for four minutes using a crusher (Huangdai 800Y, Zhejiang Yongkang Platinum Metal Products Co., Ltd., China) and dried before use. All other chemicals were used as received.

General measurements. ^{1}H-nuclear magnetic resonance (^{1}H NMR) and ^{13}C-nuclear magnetic resonance (^{13}C NMR) spectra were recorded by a BRUKER AVANCEIII 500 M spectrometer using deuterated dimethyl sulfoxide (DMSO-d6) or deuterated chloroform ($CDCl_3$) as solvent. Chemical shifts (δ) are reported in ppm relative to residual solvent signals (DMSO-d6: 2.50 ppm for ^{1}H NMR, 40.0 ppm for ^{13}C NMR; $CDCl_3$: 7.27 ppm for ^{1}H NMR). Electrospray ionization mass spectroscopy (ESI-MS) was recorded on a Bruker MicroQ-II mass spectrometer. X-ray photoelectron spectroscopy (XPS) were recorded using a Kratos AXIS Supra+ instrument. For the degraded PUF particle, thorough cleaning with THF is required prior to XPS testing to eliminate excess oxime. Fourier transform infrared (FTIR) spectra were recorded on a Bruker Vertex 70 V made by Germany. Differential scanning calorimetry (DSC) was performed on a DSC Q2000 at a heating rate of 5 °C/min under a nitrogen atmosphere (50 mL/min). The thermal gravimetric analysis (TGA) was performed on a TGA Q500 at a heating rate of 5 °C/min under nitrogen atmosphere (50 mL/min). Compressive tests were performed on a universal testing machine (SUNS, China). Gel fraction tests were conducted though solvent extraction in THF for 24 h and vacuum-drying at 50 °C for 2 h. The sample morphologies were characterized with a scanning electron microscope (SEM; Hitachi, S-4800, Japan). The porosity (*P*) of the foam was calculated using the following Eq. (1):

$$P = (1 - \rho_1/\rho_2) \times 100\% \quad (1)$$

where ρ_1 and ρ_2 are the densities of the foam and polyurethane (1.2 g/cm^3), respectively.

Model compound experiments

Model compound experiments were conducted to reveal the degradation reactions of PUF. To do so, three small molecular compounds containing urea, urethane, and biuret moieties were synthesized. Their degradation behaviors including the degradation products and the kinetics were investigated as below. To make it easier to operate, herein liquid 2-butanone oxime, an acetoxime analogue, was used. In addition, oxime-urethane, a small molecular compound generated from the three degradation reactions, was also synthesized as follows to serve as an important reference to reveal the degradation reactions and the kinetics.

Synthesis of the model compound oxime-urethane. 2-Butanone oxime (3.48 g, 40 mmol) was dissolved in THF (20 mL). Next, *p*-tolyl isocyanate (5.32 g, 40 mmol) was added dropwise to the solution with magnetic stirring. After reaction at room temperature for 20 h followed by vacuum drying at 50 °C for 6 h, oxime-urethane was obtained. The structure of the oxime-urethane was confirmed by ^{1}H NMR, ^{13}C NMR, and mass spectra analyses (Supplementary Fig. 1). ^{1}H NMR (500 MHz, DMSO-d6, ppm) δ 9.5 (m, 1H), 7.5-7.0 (m, 4H), 2.5-2.3 (m, 2H), 2.25 (s, 3H), 1.98 (m, 3H), 1.09 (m, 3H). ^{13}C NMR (126 MHz, DMSO-d6, ppm) δ 166.55, 165.85, 152.50, 136.46, 132.28, 129.62, 119.45, 28.91, 23.47, 20.80, 19.32, 15.15, 10.98, 10.37. ESI-MS Calcd for $C_{12}H_{16}O_2N_2Na$ $[M+Na]^+$: 243.1104, Found: 243.1100, Error: 0.0004 ppm.

Synthesis of the model compound 1,3-di-*p*-tolylurea. *p*-Toluidine (1.07 g, 10 mmol) was dissolved in THF (10 g). Next, *p*-tolyl isocyanate (1.33 g, 10 mmol) was added dropwise to the solution with magnetic stirring. After reaction at room temperature for 10 min followed by filtrating, washing (using THF) and vacuum drying (room temperature,

24 h) the generated precipitate, 1,3-di-*p*-tolylurea was obtained. The structure of the 1,3-di-*p*-tolylurea was confirmed by ^{1}H NMR, ^{13}C NMR, and mass spectra analyses (Supplementary Fig. 2). ^{1}H NMR (500 MHz, DMSO-d6, ppm) δ 8.5 (s, 2H), 7.5-7.0 (m, 8H), 2.24 (s, 6H). ^{13}C NMR (126 MHz, DMSO-d6, ppm) δ 153.09, 137.70, 130.96, 129.62, 118.68, 20.80. ESI-MS Calcd for $C_{15}H_{16}ON_2Na$ $[M+Na]^+$: 263.1155, Found: 263.1150, Error: 0.0005 ppm.

Synthesis of the model compound octyl *p*-tolylcarbamate. 1-Octanol (1.3 g, 10 mmol) was dissolved in toluene (5 g). Next, *p*-tolyl isocyanate (1.33 g, 10 mmol) was added dropwise to the solution with magnetic stirring. After reaction at 80 °C for 3 h followed by vacuum drying at room temperature for 24 h, octyl *p*-tolylcarbamate was obtained. The structure of the octyl *p*-tolylcarbamate was confirmed by ^{1}H NMR, ^{13}C NMR, and mass spectra analyses (Supplementary Fig. 3). ^{1}H NMR (500 MHz, DMSO-d6, ppm) δ 9.5 (s, 1H), 7.5-7.0 (m, 4H), 4.05 (m, 2H), 2.24 (s, 3H), 1.7-0.8 (m, 15H). ^{13}C NMR (126 MHz, DMSO-d6, ppm) δ 154.11, 137.16, 131.50, 129.54, 118.63, 64.47, 31.69, 29.14, 29.12, 29.05, 25.87, 22.55, 20.78, 14.41. ESI-MS Calcd for $C_{16}H_{25}O_2NNa$ $[M+Na]^+$: 286.1778, Found: 286.1772, Error: 0.0006 ppm.

Synthesis of the model compound 1,3,5-tri-*p*-tolylbiuret. 1,3-Di-*p*-tolylurea (2.4 g, 10 mmol) and *p*-tolyl isocyanate (10.64 g, 80 mmol) were mixed and reacted at 130 °C for 6 h with magnetic stirring. During the reaction, the mixture was gradually transformed from its initial immiscible paste into a homogeneous and transparent solution. After reaction for 6 h and removing the excess *p*-tolyl isocyanate by rotary evaporation at 90 °C for 2 h in vacuum, 1,3,5-tri-*p*-tolylbiuret was obtained. The structure of the 1,3,5-tri-*p*-tolylbiuret was confirmed by ^{1}H NMR, ^{13}C NMR, and mass spectra analyses (Supplementary Fig. 4). ^{1}H NMR (500 MHz, DMSO-d6, ppm) δ 9.6 (s, 2H), 7.5-7.0 (m, 12H), 2.37 (s, 3H), 2.25 (s, 6H). ^{13}C NMR (126 MHz, DMSO-d6, ppm) δ 154.14, 138.12, 136.02, 135.11, 133.21, 130.48, 129.78, 129.47, 121.49, 21.28, 20.88. ESI-MS Calcd for $C_{23}H_{23}O_2N_3Na$ $[M+Na]^+$: 396.1683, Found: 396.1676, Error: 0.0007 ppm.

Chemical degradation of 1,3-di-*p*-tolylurea. 1,3-di-*p*-tolylurea was dried, and then 2-butanone oxime was added to react at 130 °C for predetermined times. The molar ratio of urea/oxime was set as 3:46. The degradation reaction pathway of 1,3-di-*p*-tolylurea is shown in Supplementary Fig. 5. ^{1}H NMR analyses of the degradation mixture at different degradation times allows quantitative monitoring of the reaction (Supplementary Fig. 6).

Chemical degradation of octyl *p*-tolylcarbamate. Octyl *p*-tolylcarbamate was dried and 2-butanone oxime was added to react at 130 °C for predetermined times. The molar ratio of tolylcarbamate/oxime was set as 1:46. The degradation reaction pathway of octyl *p*-tolylcarbamate is shown in Supplementary Fig. 7. Again, ^{1}H NMR analyses at different reaction times are used for quantitative monitoring of the reaction (Supplementary Fig. 8).

Chemical degradation of 1,3,5-tri-*p*-tolylbiuret. 1,3,5-tri-*p*-tolylbiuret was dried and 2-butanone oxime was added to react at 130 °C for predetermined times. The molar ratio of biuret/oxime was set at 0.2:46. The degradation reaction pathway of 1,3,5-tri-*p*-tolylbiuret is shown in Supplementary Fig. 9. Again, ^{1}H NMR analyses at different reaction times are used for quantitative monitoring of the reaction (Supplementary Fig. 10).

Chemical degradation of PUF predicted from the model compounds. As PUF is degraded into particles, the low degradation degree and its complex molecular structure make it difficult to directly quantify the extent of degradation via common tests. We therefore used the data from the model compound study presented in Supplementary Figs. 6b, 8b, and 10b for prediction. These data were compounded together to predict the chemical degradation of PUF according to their original ratio in the PUF.

Reconstruction of new foams using the degradation products

The degradation mixture (containing PUF particles and acetoxime) was poured into a silicone mold immediately after the degradation. After cooling at room temperature for 24 h, the solidified sample was demolded and placed in a preheated vacuum drying oven with programmed temperatures (90, 110, 130, and 150 °C). The system was rapidly evacuated to 130 Pa, and vacuum evaporation was sustained until mass equilibrium (no detectable weight change) was achieved. The process was terminated at this stage, yielding the regenerated foam.

Life cycle assessment (LCA)

We define our recycling process as Process #1 and the classical glycolysis recycling process[6,9] as Process #2. For life cycle assessment (LCA), the system boundary was determined from the waste commercial PUF to new PUF. The target products were set with a same value of 1.000 kg. The data relating to the PUF end-of-life processes were derived from Ecoinvent database (version 3.5) in Simapro software, which employed the allocation at point of substitution (APOS), cut-off by classification, and consequential data[22,23]. The process data were converted to environmental information, including fossil depletion, human toxicity, terrestrial ecotoxicity, marine ecotoxicity, ozone depletion, and eutrophication potential through life cycle impact assessment (LCIA). The corresponding LCA network structure was presented in Supplementary Fig. 19, and the compared normalized results were shown in Supplementary Tables 1–3.

Techno-economic analysis

The total direct manufacturing costs for process #1 and process #2, including the material and energy, are $0.59/kg and $2.06/kg, respectively. Other costs including equipment, labor and R&D are difficult to estimate, but are expected to be minor for high volume production. The detailed cost estimates are presented as follows.

Analysis of the material cost. Herein, the PUF waste cost is assumed as $0/kg based on its waste nature. The material cost for process #1 is also assumed as $0/kg based on the fact that the acetoxime is inexpensive and fully recovered, but the corresponding recovering cost is estimated in form of energy in the next section. The material cost for process #2 is summarized in Supplementary Table 4, and the corresponding total material cost is estimated at around $2.02/kg.

Analysis of the energy cost. The process and energy consumption for converting PUF waste into new PUF is presented in Supplementary Fig. 19. The energy consumption is estimated below:

In the reaction or separation step, the enthalpy change (ΔH) is mainly assigned to the temperature variation, and/or reagent (acetoxime or ethylene glycol) evaporation. Therefore ΔH is calculated as the following Eq. (2):

$$\Delta H = \Delta H_t + \Delta H_p = mC\Delta T + \Delta H_p \quad (2)$$

where ΔH_t is the enthalpy of temperature variation. ΔH_p is the enthalpy of phase change (evaporation). m, C and ΔT are assigned to the mass of the reaction system, specific heat capacity and temperature variation, respectively. The source of the thermodynamic data are presented in Supplementary Table 5.

In addition, the energy efficiency in the whole process is conservatively set at 50-80%. Accordingly, the total energy consumption for process #1 is calculated as 21133.1 kJ/kg (5.870 kW·h/kg) and the corresponding energy cost is calculated as $0.5870/kg with an

electricity price of $0.1/kW·h. The total energy consumption for process #2 is calculated as 1437.5 kJ/kg (0.399 kW·h/kg) and the corresponding energy cost is calculated as $0.0399/kg.

Data availability

The data that support the findings of this study are available as Source data Figs. 2–4 and Supplementary data set. They are also available via Figshare (https://doi.org/10.6084/m9.figshare.28862105). Source data are provided with this paper. All data are available from the corresponding author upon request. Source data are provided with this paper.

References

1. Plastics Europe. Plastics - the fast facts. Available online: https://plasticseurope.org/knowledge-hub/plastics-the-fast-facts-2023/ (2023).
2. Deng, Y. et al. Reviewing the thermo-chemical recycling of waste polyurethane foam. *J. Environ. Manage.* **278**, 111527 (2021).
3. Bandegi, A., Montemayor, M. & Manas-Zloczower, I. Vitrimerization of rigid thermoset polyurethane foams: a mechanochemical method to recycle and reprocess thermosets. *Polym. Adv. Technol.* **33**, 3750–3758 (2022).
4. Liu, Z. et al. Chemical upcycling of commodity thermoset polyurethane foams towards high performance 3D photo-printing resins. *Nat. Chem.* **15**, 1773–1779 (2023).
5. Post, W., Susa, A., Blaauw, R., Molenveld, K. & Knoop, R. J. I. A review on the potential and limitations of recyclable thermosets for structural applications. *Polym. Rev.* **60**, 359–388 (2020).
6. Simon, D., Borreguero, A. M., De Lucas, A. & Rodriguez, J. F. Recycling of polyurethanes from laboratory to industry, a journey towards the sustainability. *Waste Manage.* **76**, 147–171 (2018).
7. Purwanto, N. S., Chen, Y. & Torkelson, J. M. Reprocessable, bio-based, self-blowing non-isocyanate polyurethane network foams from cashew nutshell liquid. *ACS Appl. Polym. Mater.* **5**, 6651–6661 (2023).
8. Banik, J., Chakraborty, D., Rizwan, M., Shaik, A. H. & Chandan, M. R. Review on disposal, recycling and management of waste polyurethane foams: a way ahead. *Waste Manage. Res.* **41**, 1063–1080 (2023).
9. Heiran, R. et al. Glycolysis: an efficient route for recycling of end of life polyurethane foams. *J. Polym. Res.* **28**, 22 (2021).
10. Feng, H. J. et al. Ultratough yet dynamic crystalline poly(thiourethane) network directly from low viscosity precursors. *CCS Chem.* **6**, 682–692 (2024).
11. Qin, B. & Zhang, X. On depolymerization. *CCS Chem.* **6**, 297–312 (2024).
12. Sheppard, D. T. et al. Reprocessing postconsumer polyurethane foam using carbamate exchange catalysis and twin-screw extrusion. *ACS Cent. Sci.* **6**, 921–927 (2020).
13. Kim, S., Li, K., Alsbaiee, A., Brutman, J. P. & Dichtel, W. R. Circular reprocessing of thermoset polyurethane foams. *Adv. Mater.* **35**, 2305387 (2023).
14. Delebecq, E., Pascault, J. P., Boutevin, B. & Ganachaud, F. On the versatility of urethane/urea bonds: reversibility, blocked isocyanate, and non-isocyanate polyurethane. *Chem. Rev.* **113**, 80–118 (2013).
15. Liu, M. et al. Oxime-based and catalyst-free dynamic covalent polyurethanes. *J. Am. Chem. Soc.* **139**, 8678–8684 (2017).
16. Wicks, D. A. & Wicks, J.rZ. W. Blocked isocyanates III: Part B: uses and applications of blocked isocyanates. *Prog. Org. Coat.* **41**, 1–83 (2001).
17. Guo, L. et al. Recycling of flexible polyurethane foams by regrinding scraps into powder to replace polyol for re-foaming. *Materials* **15**, 6047 (2022).
18. Zhou, T. Boiler cleaning method. CN Patent 105987372 (2016).
19. Jeon, H. G., Inoue, M., Hirarnatsu, N., Ichikawa, M. & Taniguchi, Y. A modified sublimation purification system using arrays of partitions. *Org. Electron.* **9**, 903–905 (2008).
20. Bhatta, S., Janezic, T. S. & Ratti, C. Freeze-drying of plant-based foods. *Foods* **9**, 87 (2020).
21. Silva, M. C. et al. Digital sublimation printing on knitted polyamide 6.6 fabric treated with non-thermal plasma. *Polymers* **13**, 1969 (2021).
22. Dones, R., Heck, T., Faist Emmenegger, M. & Jungbluth, N. Life cycle inventories for the nuclear and natural gas energy systems, and examples of uncertainty analysis. *Int. J. Life Cycle Ass.* **10**, 10–23 (2005).
23. Hischier, R. & Baudin, I. LCA study of a plasma television device. *Int. J. Life Cycle Ass.* **15**, 428–438 (2010).

Acknowledgements

This work is supported by National Natural Science Foundation of China (Nos. U23A2098, 22288102, and 52033009 to T.X.).

Author contributions

T.X. and Z.L. conceived the concept. T.X. and Y.Z. supervised the project. Z.L., L.L. and Y.L. designed and performed the experiments. K.Y., S.L., and W.L. conducted the life cycle assessment. T.X. and Z.L. wrote the manuscript. All authors participated in result analysis and discussion.

Competing interests

The authors declare no competing interests.

Additional information

Supplementary information The online version contains supplementary material available at https://doi.org/10.1038/s41467-025-60111-x.

Correspondence and requests for materials should be addressed to Yutian Zhu or Tao Xie.

Peer review information *Nature Communications* thanks Pere Verdugo Fernández and the other, anonymous, reviewer(s) for their contribution to the peer review of this work. A peer review file is available.